

Dielectric relaxation in hydroxyethyl cellulose

K. Liedermann^{a,*}, L. Lapčák Jr.^b

^aDepartment of Physics, Faculty of Electrical Engineering and Computer Science, Technical University of Brno, Technická 8, CZ-61600 Brno, Czech Republic

^bDepartment of Physics and Material Engineering, Faculty of Technology, Technical University of Brno, Náměstí TGM 275, CZ-762 72 Zlín, Czech Republic

Received 7 April 1999; received in revised form 9 August 1999; accepted 16 September 1999

Abstract

This paper presents the results of the dielectric analysis of hydroxyethyl cellulose (HEC) in the temperature range 100–350 K and in the frequency range 20 Hz–1 MHz. The results show a distinct broad relaxation process in the temperature range 150–250 K with activation energy of about 33.4 MJ/kmol. The strength of the relaxation, $\epsilon_s - \epsilon_\infty$, increases only slightly with temperature and the apparent increase of the height of the relaxation maximum is attributed to an increase of the co-operativity parameter α . This increase of α is interpreted as decrease of the co-operativity of dipole motions with increasing temperature. The origin of the relaxation is ascribed to the reorientation of double ethylene oxide groups or part of these. © 2000 Elsevier Science Ltd. All rights reserved.

Keywords: Dielectric relaxation; Hydroxyethyl cellulose; Hydrogen bridges; Molecular dynamics

1. Introduction

Polysaccharides of various compositions are being increasingly used in medicine and biology, e.g. as substitute materials for human bodies or protective coatings for drugs. For these purposes, it is desirable to provide a comprehensive characterisation of a given material.

One of the methods to characterise materials is based on the analysis of their dielectric spectra. Dielectric analysis provides the information about the motion of entities having an electric charge or an electric dipole moment, i.e. about dipole reorientation, rotations of the main and segmental chains and conductivity mechanisms.

In dielectric relaxation spectroscopy (DRS), the basic quantity measured is the complex admittance Y of the sample under test. The dimension-independent quantity, complex permittivity ϵ , is obtained as

$$\epsilon = Y/(j\omega C_0)$$

where C_0 is the geometric capacitance of the sample, ω is angular frequency of the excitation voltage and j is $\sqrt{-1}$. The total complex permittivity may then be generally expressed as a sum of individual conductivity and relaxation components:

$$\epsilon = \sum \epsilon_{(\text{cond})} + \sum \epsilon_{(\text{relax})}$$

$\epsilon_{(\text{cond})}$ and $\epsilon_{(\text{relax})}$ being the individual conductivity and

relaxation components, respectively. The conductivity component is then due to the motion of free charge carriers, or more generally of charge carriers travelling at long distances, whereas the relaxation component is due to the motion of bound charge carriers and dipoles. As the electric dipoles in a molecule lie along chemical bonds, the relaxation part provides the information about the molecular dynamics of polymer segments. Complex permittivity may be measured as a function of frequency at different temperatures (El-Shafee, 1996) or as a function of temperature at different frequencies (Kim, Kim & Nishinari, 1991; Montés & Cavaillé, 1999; Montés, Mazeau & Cavaillé, 1997). The advantages and disadvantages of both approaches are discussed in more detail in Hedvig, 1984. In this research, permittivity was measured as a function of frequency at different temperatures, as in such a case it was possible to proceed to much lower frequencies (down to 10^{-5} Hz) through the time-domain DRS.

Molecular mobility of the HEC parent structure, cellulose, has been recently examined both by mechanical (Montés et al., 1997) and dielectric (Montés & Cavaillé, 1999) relaxation spectroscopy at constant frequency and variable temperature. As only sub- T_g relaxations were examined, α -relaxation was thus excluded from the analysis. Mechanically (Montés et al., 1997), two relaxations were observed, β and γ , with activation energies $E_{a\beta} = 85$ MJ/kmol and $E_{a\gamma} = 40$ MJ/kmol and pre-exponential relaxation times $\tau_{0\beta} = 10^{-20}$ s and $\tau_{0\gamma} = 10^{-20}$ s, respectively. Mechanical β relaxation is ascribed to the motion

* Corresponding author.

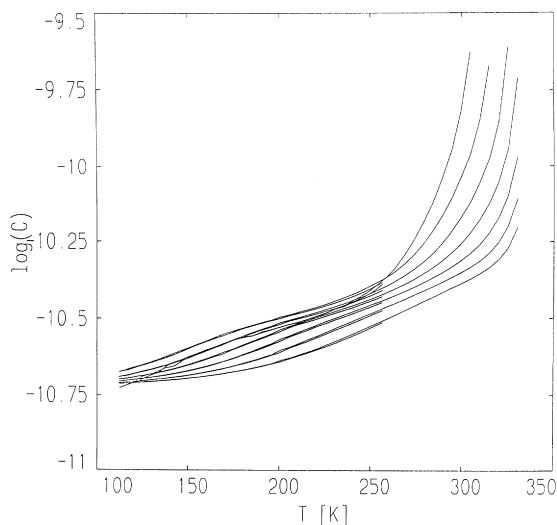


Fig. 1. Temperature dependence of capacitance for various frequencies, top: 20 Hz, bottom: 1 MHz.

of main chain segments and the values of E_a and τ_0 suggest a high degree of co-operativity, whereas the γ relaxation is interpreted as being due to the rotation of primary hydroxyl groups (i.e. hydroxyl groups attached to the glucose ring via the $-\text{CH}_2-$ methylene group); this sort of motion is localised and is not associated with any conformational changes in the main chain.

Dielectrically, only one rather broad relaxation was observed in cellulose (Montés & Cavaillé, 1999). As the DRS is based on the motion of dipoles or electric charges, it need not reproduce the motion of the main chain segment (particularly if the chain segment has low dielectric activity, hence the mechanical β relaxation need not be observed dielectrically at all. Therefore the dielectric relaxation observed was also ascribed to the motion of hydroxyl groups, this time both primary and secondary ones, and is

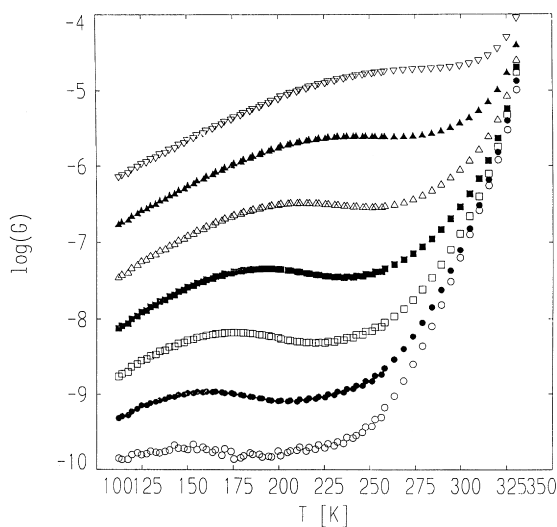


Fig. 2. Temperature dependence of conductivity at various frequencies (○: 20 Hz, ▽: 1 MHz).

referred to again as the γ relaxation. The apparent activation energy $E_a = 50$ MJ/kmol is not very different from the value of the activation energy obtained from mechanical spectroscopy, however, the relaxation time $\tau_{\text{odiel}} = 10^{-17}$ s differs significantly from $\tau_{0\gamma\text{mech}} = 10^{-12}$ s. In contrast to mechanical relaxation, both types of hydroxyl groups are active, so that it is possible to separate the contributions of primary and secondary hydroxyl groups, the parameters of individual components being $E_{a\gamma\text{OH}} = 32$ MJ/kmol, $\tau_{0\gamma\text{OH}} = 5.10^{-15}$ s and $E_{a\gamma\text{CH}_2\text{OH}} = 34$ MJ/kmol, $\tau_{0\gamma\text{CH}_2\text{OH}} = 9.10^{-13}$ s, respectively. The latter is close to the values obtained for the mechanical γ relaxation.

Relaxation properties of hydroxyethyl cellulose were investigated both mechanically and dielectrically by Kim et al. (1991), again at constant frequency against varying temperature. The origin of the relaxation is attributed to the rotation of CH_2OR , groups, where $\text{R} = \text{H}$ or $-(\text{CH}_2\text{CH}_2\text{O})_m-\text{H}$ and/or to the rotation of ethylene oxide groups substituted on secondary hydroxyl groups in the glucosidic chain. Unfortunately, no data on activation energy or pre-exponential relaxation times are provided in (Kim et al., 1991).

Carboxymethyl cellulose (CMC) and its sodium salt (NaCMC), was investigated dielectrically by El-Shafee (1996). The origin of the relaxation seen was the rotation of carboxymethyl ($-\text{OCH}_2\text{COOH}$) groups with a high activation energy of 120 MJ/kmol (CMC) and 111 MJ/kmol (NaCMC). The slightly higher value of the activation energy in CMC is interpreted as a evidence for hydrogen bonding between neighbouring parallel chains.

HEC is just one of the many polysaccharides currently investigated by this group. Other polysaccharides include CMC mentioned above, chondroitin sulphate (CHS) and hyaluronic acid (HYA). The results of measurements on CMC, HYA and CHS will be reported later.

2. Experimental

Samples of HEC Natrosol 250 HHR (Aqualon) were supplied in the form of self-supporting films of thickness 0.15 mm. Samples were rinsed for 24 h in pure ethanol to be free from any absorbed water, and then kept in an desiccator with silicagel under vacuum. Prior to measurements the samples were provided with 4-point silver paint electrodes of an area of about 1 cm^2 .

The measurements were made using the HP 4284A LRC analyser and the Novocontrol Quattro system using a cryostat with liquid nitrogen cooling. The frequency range available was 20 Hz–1 MHz.

The sample to be tested was connected with thin copper wires to the sample holder which was inserted into the cryostat and then heated in the nitrogen stream up to 330 K (without any impedance being measured) so as to remove any traces of water which might still be present or picked by the sample during manipulation. The temperature was then

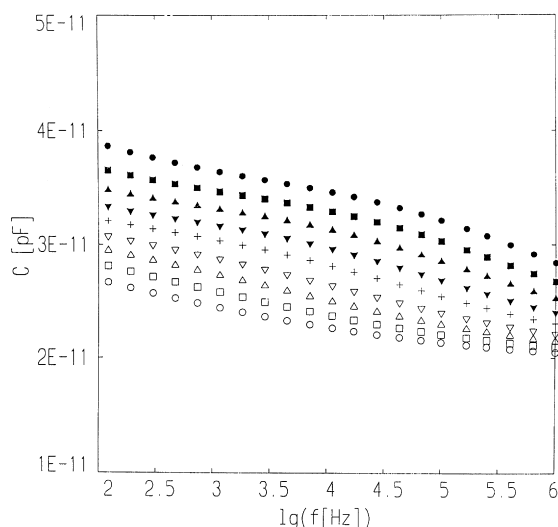


Fig. 3. Frequency dependence of capacitance at 10 K steps (○: 160 K, ●: 242 K).

decreased in regular 5 K steps down to 100 K and the frequency sweep was carried out at individual temperature settings. After reaching the minimum temperature of 100 K the temperature was increased again in 5 K steps and the impedance measurement was repeated. The measurement was terminated once the temperature in the cryostat reached the level of the room temperature (295 K). The measurement at both decreasing and increasing temperatures was performed to observe any temperature hysteresis.

3. Results

The results of the measurements were the frequency and temperature dependence of complex admittance $Y = j\omega C + G$, which were at a later time converted into the complex permittivity ϵ . The temperature dependence of capacity C and conductivity G is shown for different frequencies in Figs. 1 and 2. The curves on heating and cooling are not quite identical, however we consider the origin of this difference to be due rather to the thermal inertia of the measuring system (there was a distance of some 5 mm between the temperature sensor and the sample) rather than to a particular physical phenomenon.

Temperature plots cannot be fitted to equations containing parameters, which have physical meaning, however, there are a number of theories (Böttcher & Bordewijk, 1978; Jonscher, 1983) predicting time response of a dielectric to the application of an external electric field. Frequency plots are just Fourier transforms of the time response data. These frequency plots are often more informative than temperature plots, as the parameters obtained from the frequency plots may be related to theory and hence can have a physical meaning (Chamberlin, Bohmer, Sanches & Angell, 1992). Therefore, in the following the results will be presented as frequency plots. The plots of

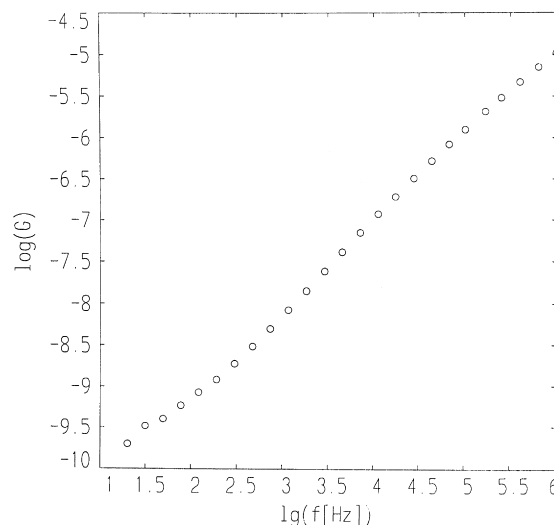


Fig. 4. Frequency plot of conductivity at $T = 211$ K (inflection point of the S-shaped curve shifts with the increasing temperature towards higher frequencies, so that plotting more curves on a single graph in a similar way as in Figs. 1–3 would result in a large number of overlapping lines).

capacitance, C , and conductivity, G , vs. frequency, f , are given in Figs. 3 and 4.

From the DRS viewpoint the most important quantity used for the description of the relaxation phenomena is not the conductivity G , but the imaginary part of the dimensionless complex permittivity $\epsilon''(\omega)$, often referred to as the dielectric spectrum. It can be readily shown that:

$$\epsilon''(\omega) = G/(\omega C_0) = kG/f$$

where k is a constant involving sample dimensions and a numerical factor of 2π . The plots of $\epsilon''(\omega)$ at various temperatures are given in Fig. 5. Apparently, the $\epsilon''(\omega)$ curve exhibits a maximum that shifts to higher frequencies with increasing temperature until it completely vanishes from the experimentally available frequency window at about 250 K. On decreasing temperature, the relaxation maximum shifts towards lower frequencies and before leaving the experimentally available frequency window it gradually merges with the AC conductivity component at low frequency, which implies that the activation energy of the conductivity process is lower than that of the relaxation process.

4. Discussion

The dielectric spectra shown in Fig. 5 were analysed under the assumption that they are due to one conductivity process and a single broad relaxation process. It is possible to fit say, one conductivity process and two relaxation processes, but without strong evidence for the presence of two relaxation processes this approach might lead to a false interpretation, as the fit algorithm is able to find an acceptable match for a wide variety of fit functions.

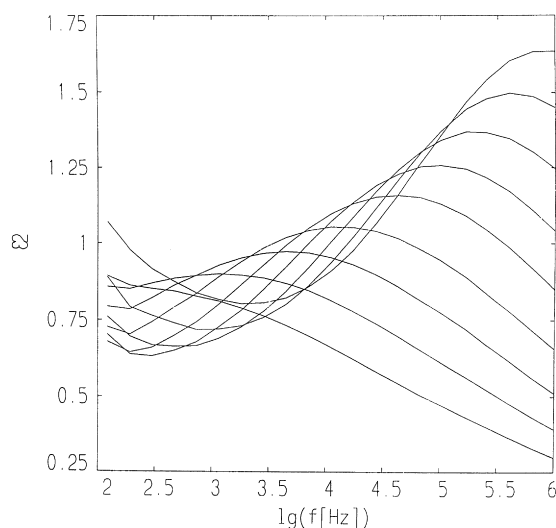


Fig. 5. Frequency dependence of $\epsilon''(\omega)$ at 10 K steps (from 160 up to 242 K).

The conductivity process was modelled using the empirical formula (Jonscher, 1983):

$$\epsilon''(\text{cond})(\omega) = A\omega^n$$

whereas the relaxation was modelled using the well-known Havriliak–Negami formula (Havriliak & Negami, 1967):

$$\hat{\epsilon}(\bar{\omega}) = \epsilon_\infty + \frac{\epsilon_s - \epsilon_\infty}{(1 + (j\omega\tau_0)^\alpha)^\beta}$$

Best fits of the sum of both components to the measured values were found using the DK software, version 3.6, developed at the Max Planck Institute for the Polymer Research, Mainz, Germany. The software is based upon the Marquardt–Levenberg algorithm of the non-linear least-squares (gradient method) and it allowed to model up to 3 relaxation processes and 2 conductivity processes, i.e. it might yield up to 16 parameters.

In the above formula α gives the left (i.e. low-frequency)

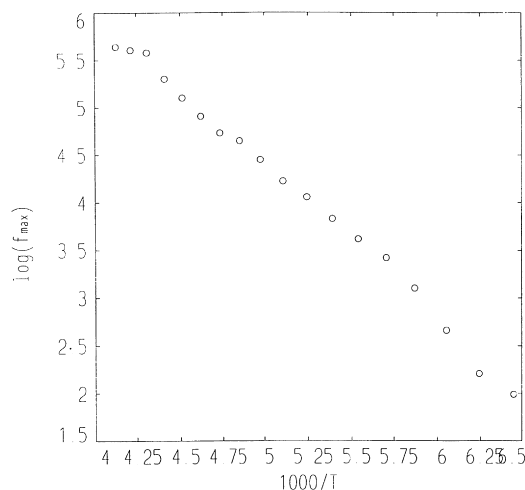


Fig. 6. Activation plot $\log(f_{\max}) = f(1/T)$.

slope of the relaxation, the product $\alpha\beta$ gives the right (i.e. high-frequency) slope of the relaxation, $\epsilon_s - \epsilon_\infty = \Delta\epsilon$ indicates the strength of the relaxation (i.e. the height of the relaxation peak) and τ_0 corresponds to the position of the relaxation peak on the frequency axis. The position of the relaxation peak f_{\max} is related to τ_0 by a simple formula:

$$f_{\max} = 1/(2\pi\tau_0)$$

The temperature dependence of the relaxation frequency is best shown in the so-called activation plot, $\log(f_{\max})$ vs. $1/T$ in Fig. 6. An example of what the relaxation spectrum together with the fitted conductivity and relaxation processes looks like is shown in Fig. 7 (HECD22).

The activation plot may be approximated with a straight line, which means that the relaxation follows the Arrhenius law with activation energy $E_a = (33.2 \pm 0.4)$ MJ/kmol and pre-exponential factor (relaxation time formally at infinite temperatures) $\tau_0 = 1.25 \times 10^{-4}$ s. The straight line suggests that the origin of the relaxation should be seen in individual rearrangements of single non-interacting dipoles rather than in collective behaviour of co-operating species which is likely to correspond to the Vogel–Fulcher–Tamman law. As the rearrangement of dipole moments associated with oxygen atoms lying in the main chain would necessitate a strongly collective behaviour, which in the activation plot manifests as a bending curve approaching the Vogel–Fulcher–Tamman transition temperature T_0 , the origin of the currently observed relaxation is due rather to the motion of dipoles exhibiting much less co-operativity, i.e. dipoles lying in side groups. In the case of HEC, such dipoles are formed either by the secondary hydroxyl groups attached to the main chain or by much longer double ethylene oxide groups.

Besides the activation plot, $\log(f_{\max})$ vs. $1/T$, the behaviour of other fitted parameters, namely α , $\alpha\beta$ and $\Delta\epsilon$, with varying temperature was also analysed; according to Feldman (1995), parameter β alone does not have any particular physical interpretation whereas the product $\alpha\beta$ does. The values of $\Delta\epsilon$ and of the product $\alpha\beta$ may be used for the analysis only up to 220 K, as above 220 K they exhibit considerable scatter. This is due to the fact that the relaxation peak starts to disappear from the experimental frequency window so that the determination of the height of the maximum as well as that of the right slope of the peak is less accurate. On the contrary, the left slope of the relaxation peak remains further within the experimental window and thus the determination of its value (α) did not present any problem.

In addition to the above, the temperature dependencies of α , $\alpha\beta$ and $\Delta\epsilon$ may be summed up as a steady increase of α with increasing temperature from 0.25 at 150 K to 0.5 at 250 K, a moderate increase of $\Delta\epsilon$ with increasing temperature from 0.78 at 150 K to about 0.87 at 220 K and an almost temperature-independent value of the product $\alpha\beta$ (about 0.25–0.3) in the temperature range 150–220 K. According to Feldman (1995), α is related to the strength of co-operative

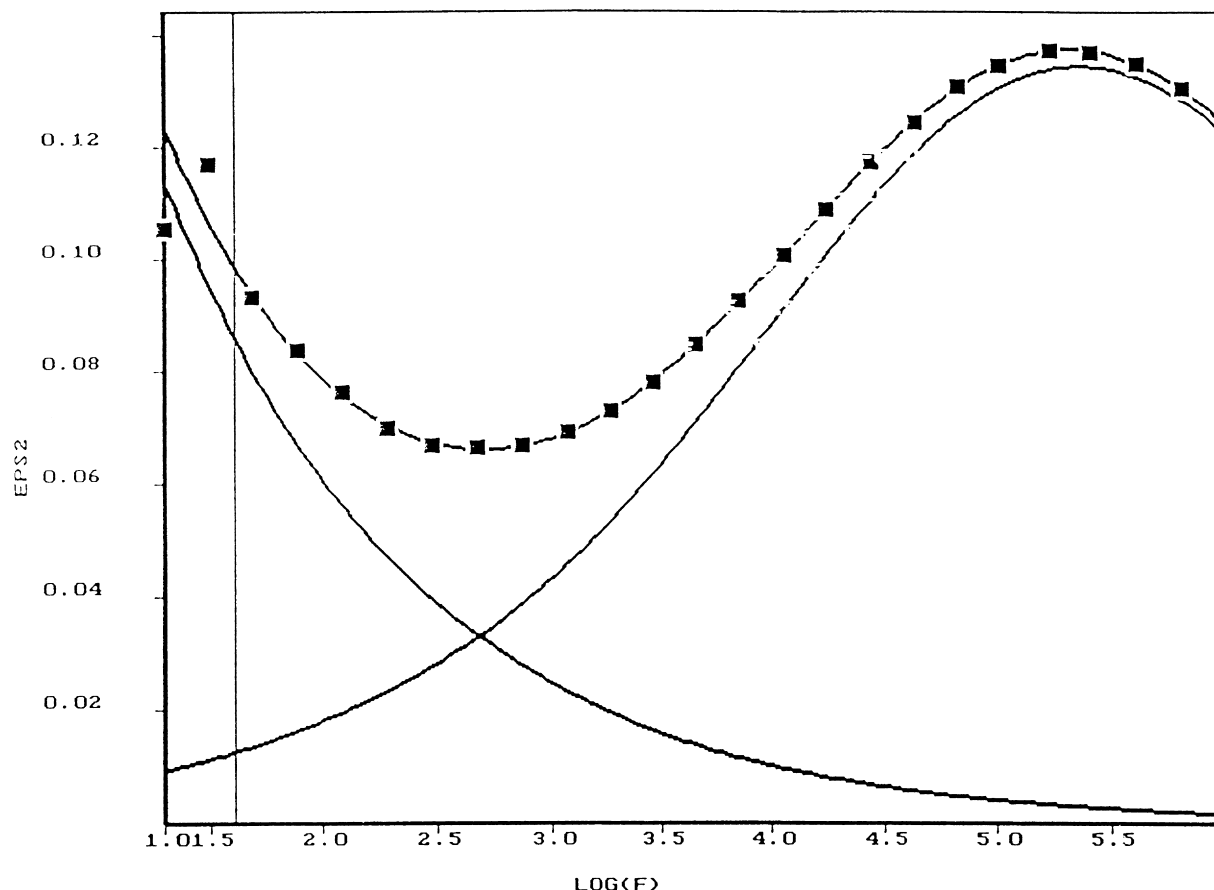


Fig. 7. Frequency dependence of ϵ'' for the sample HECD22 ($T = 221.5$ K) with fitted conductivity and relaxation processes shown.

interactions of corresponding dipoles (lower values of α correspond to a stronger co-operativity). Therefore it might be proposed that the relaxation observed is brought about by the reorientation of double ethylene oxide groups, as the individual secondary hydroxyl groups lie far apart and thus the possibility of their mutual interactions is reduced. The increase of α with temperature indicates decreasing co-operativity of the dipole movement which can be attributed to the intensification of thermal motions of double ethylene oxide groups and thus to the weakening of their mutual interactions. The steric hindrances, whose measure is the product $\alpha\beta$, remain apparently temperature independent.

As for $\Delta\epsilon$, if the relaxation is dipolar by nature, one would expect a decrease with increasing temperature according to Curie's law ($\Delta\epsilon \sim 1/T$) (Okadzaki, 1979), which is contrary to the dependence observed. A possible explanation is suggested by El-Shafee (1996) and Chamberlin et al. (1992): the magnitude of $\Delta\epsilon$ is proportional not only to the dipole concentration and dipole moment, but it is also governed by the inter-chain interactions between adjacent chains, possibly due to hydrogen bonds. These interactions become weaker with increasing temperature so that the decrease of the effective dipole moment due to Curie's law is more than balanced by the diminishing inter-chain constraints, which effectively hindered re-orientations of

the hydroxyl groups. Consequently, a moderate net increase of $\Delta\epsilon$ with increasing temperature is seen.

It is worth comparing the above conclusions with those of Montés and Cavaillé (1999) and Kim et al. (1991). From the empirical Arrhenius curve data, the activation energy of 33.2 MJ/kmol and the pre-exponential relaxation time of 1.25×10^{-4} s result in the relaxation peak frequency $f_{\max} = 8$ Hz at the temperature -130°C , which is very close to the relaxation peak frequency 10 Hz reported by Kim et al. (1991), so that the data presented here seems to support the ideas proposed by Kim et al. (1991). However, these results also bear a close resemblance to the values of activation energy and pre-exponential relaxation times found for cellulose (Montés & Cavaillé, 1999), where no ethylene oxide groups are present. This would favour the interpretation that the relaxation is due to the secondary hydroxyl groups because they are present both in ordinary cellulose and in HEC, and the low value of α indicates strong interactions between secondary hydroxyl groups. For space reasons, however, the mutual intra-chain interactions of secondary hydroxyl groups are rather rare, and therefore it is difficult to accept the idea that they alone would account for the relatively broad relaxation peak ($\alpha = 0.25 - 0.5$, $\alpha\beta = 0.3$). Although the possibility of inter-chain interactions cannot be ruled out, it is worthwhile examining other possible explanations.

In order to examine potential causes of the observed dielectric relaxation more closely, the charge distribution and the corresponding dipole moment in the HEC side group were investigated. The calculations were performed with the commercial SPARTAN software, version 4.1a4, by WAVEFUNCTION, Inc., CA, USA. Structure optimisation was carried out by the molecular dynamics simulation (SYBYL) approach and the consecutive calculation of the charge distribution was made by the semi-empirical method RHF/AM1, both of which were implemented in the SPARTAN software. The bond angle $\cdots\text{C}-\text{O}-\text{H}$ at the terminating oxygen atom was 179.9° (virtually a straight line) and the bond angle $\cdots\text{O}-\text{C}-\text{C}\cdots$ at the middle carbon atom was 108.6° (almost identical with the angle of the standard tetrahedron). The modelling results depend on the conformer type and on the size and arrangement of the main HEC chain; therefore, the computation was repeated on a shorter segment, but the results were the same. Therefore, it can be assumed that the $\cdots\text{O}\cdots$ bonds are linear and the bonds attached to the carbon atom point to the tops of the regular tetrahedron. Partial charges on the segment end $-\text{O}-\text{C}-\text{C}-\text{O}-\text{H}$ are (from left to right) -0.59 , $+0.21$, $+0.3$, -0.8 , $+0.47$ (in units of electronic charge), partial charges of hydrogen atom attached to the hydroxyl carbon are 0.02 . Total dipole moment of the segment end is, however, only 0.1641 D. The above distribution of electric charge along the ethylene oxide unit together with a relatively small value of the total dipole moment suggest that there are dipoles inside the ethylene oxide unit which do not cancel out. Hence, the relaxation is due not only to the rotation of the hydroxyl groups but rather to the reorientation of the whole ethylene oxide unit. In such a case the relaxation strength should increase with the increasing concentration of ethylene oxide units, which was actually reported by Kim et al., 1991. The width of the relaxation is then due to the co-operative character of the reorientation brought about by the large size of the double ethylene oxide units and to the presence of inter-chain bonding by hydrogen bridges.

5. Conclusion

The origin of the relaxation in the hydroxyethyl cellulose is interpreted as being due to the reorientation of the double ethylene oxide groups constrained by their large size and inter-chain bonding by hydrogen bridges. The apparent

activation energy was $E_a = (33.4 \pm 0.2 \text{ MJ/kmol})$ and the relaxation process exhibited a typical Arrhenius behaviour. The increase of α (steepness of the left side of the maximum) points to decreasing co-operativity of the relaxation with temperature. To observe the relaxation due to the motions of dipoles lying in the main chain would probably require measurements at much higher temperatures (lower frequencies), where, however, relaxation phenomena are often masked by the conductivity component. On the contrary, the relaxation due to secondary hydroxyl groups is assumed to take place at higher frequencies (in the MHz to GHz range).

Acknowledgements

This work was supported by the grant No. FU470004 of the Technical University in Brno. One of the authors (K.L.) is indebted to the German Academic Exchange Service (DAAD) for providing scholarship for a study stay at the University of Augsburg. The co-operation and advice from this side is also gratefully acknowledged. Author L.L., Jr. would like to express his gratitude for partial financing of this research to Ministry of Education, Youth and Sports of Czech Republic (Grant. No. VS96108).

References

- Böttcher, C. J. F., & Bordewijk, P. (1978). *Theory of dielectric polarization. Vol. II. Dielectrics in time-dependent fields* (2nd ed.). Amsterdam: Elsevier.
- Chamberlin, R. V., Böhmer, R., Sanches, E., & Angell, C. A. (1992). *Physics Review B*, 46, 5787.
- El-Shafee, E. (1996). *Carbohydrate Polymers*, 31, 93.
- Feldman, Y. (1995). *Trends in Polymer Science*, 3, 53.
- Havriliak, S., & Negami, S. (1967). *Polymer*, 8, 161.
- Hedvig, P. (1984). *IEEE Transactions on Electrical Insulation*, 19, 371.
- Jonscher, A. K. (1983). *Dielectric relaxation in solids* (1st ed.). London: Chelsea Dielectric Press.
- Kim, K. Y., Kim, N. H., & Nishinari, K. (1991). *Carbohydrate Polymers*, 16, 189.
- Montés, H., & Cavaillé, J. Y. (1999). *Polymer*, 40, 2649.
- Montés, H., Mazeau, K., & Cavaillé, J. Y. (1997). *Macromolecules*, 30, 6977.
- Okadzaki, K. (1979). (in Russian, translated from Japanese). *Posobije po elektrotehničeskim materialam [Electrical engineering materials handbook]* (p. 432). Moskva: Izd Energija.